****

THIS PAPER HAS BEEN SUBMITTED TO BOTH THE TECHNICAL AND STUDENT CONFERENCES

****

A Novel Neutron-Gamma Dosimeter

T. Wood, B.J. Lewis, E.C. Corcoran, K. McDermott
Royal Military College of Canada, Ontario, Canada

Abstract

A novel DNA dosimeter, comprised of synthetic DNA strands suspended in water, is capable of accurate absorbed *dose-to-tissue* measurements in mixed neutron-gamma fields. When exposed to ionizing radiation, the DNA strands break releasing a fluence of visible photons. The system responds equally to all radiation types including neutron radiation. Based on theoretical analysis, the DNA dosimeter is accurate to 14% at one standard deviation when measuring an unknown spectrum of mixed neutron-gamma radiation. Linearity has been experimentally verified in gamma and x-ray fields from 100 mGy to 10 Gy and the detector's lower limit of detection is 100 mGy.

1.   Introduction

Dosimetry is an important component of the health and well-being of all workers who may be exposed to elevated levels of radiation including members of the nuclear power industry. In Canada, the Canadian Nuclear Safety Commission (CNSC) regulates the level of radiation exposure for a Nuclear Energy Worker (NEW). A NEW is required to wear a personal monitoring dosimeter when exposure to ionizing radiation is possible [1]. Common personal monitoring dosimeters include thermoluminescence dosimeters (TLDs), radiochromic film, and diodes. These devices are capable of low-dose measurements and provide accurate results when the radiation is a well characterized beta or gamma field. Neutron dosimetry is more complicated due to the presence of a secondary gamma field which results from inelastic scattering and capture reactions with the neutron source, shielding, and surrounding materials. Furthermore, the neutron and gamma energy spectra are often unknown. Mixed and unknown radiation fields, such as those present in a nuclear power plant, make accurate absorbed dose calculations difficult due to measurement and calculation error. Measurement inaccuracies occur in mixed radiation fields if the detector responds with varying sensitivities to the different types of radiation present. This is a common characteristic of TLDs and diodes which respond with a high sensitivity to beta-gamma fields but are not sensitive to neutron fields, and radiochromic film which responds to neutron fields with a sensitivity significantly lower than that of beta-gamma fields [2]. Calculation inaccuracies occur when converting between *dose-to-detector* and *dose-to-tissue* if the radiation field is not well characterised and the material in the active volume of the dosimeter is different from that of tissue. Lithium fluoride (LiF) TLDs and some forms of radiochromic film are considered tissue equivalent however microscopic differences between tissue and the dosimeter result in calculation errors when a broad energy spectrum is considered [3]. The DNA dosimeter has a better calculation accuracy than LiF TLDs or radiochromic film because its atomic composition is closer to that of tissue, and has better measurement accuracy because of hydrogen present in the active volume which makes it sensitive to neutron radiation. Microdosimetric Monte Carlo (MC) algorithms have shown that in a system similar to that of the

DNA dosimeter, the response is constant in all radiation fields implying that minimal measurement inaccuracies occur for mixed neutron-gamma measurements [4]. Moreover, the DNA dosimeter bypasses the need to convert between *dose-to-detector* and *dose-to-tissue* because the system is tissue equivalent and the two quantities are nearly equal. These characteristics contribute to the unique ability of the DNA dosimeter to accurately measure and calculate the absorbed *dose-to-tissue* from mixed neutron-gamma fields for personal monitoring purposes.

2.   Dosimetry Theory

The DNA dosimeter is comprised of single strands of DNA suspended in water, making it more tissue equivalent than LiF TLDs and radiochromic film which have similar effective atomic numbers to tissue but contain different atomic composites. This affords the DNA dosimeter more accurate *dose-to-tissue* calculations across a broad spectrum of radiation fields compared to other tissue equivalent dosimeters. Moreover, the presence of water and hydrogen in the dosimeter's active volume enables the DNA dosimeter to respond to neutron radiation and the sensitivity of the dosimeter is nearly equal for gamma and neutron particles. Thus, unlike other personal monitoring devices, the DNA dosimeter is capable of both accurately measuring absorbed dose in a broad spectrum of mixed radiation fields, and accurately calculating the desired *dose-to-tissue* quantity. According to the theory dereived in this paper, the overall *dose-to-tissue* accuracy is 14% at one relative standard deviation, which is much better than that of any other device currently used for personal monitoring.

2.1   Neutron Dosimetry

Neutrons interact with hydrogenous composites such as water and A-150 plastic considerably more than with typical dosimeter materials like ^{7}Li, F, and Si [5]. Standard LiF TLDs and silicon diodes do not respond to neutron radiation. A LiF TLD may be enriched with ^{6}Li, or a diode may be lined with ^{10}B to create alpha particles which are detectable. However, from a radiation safety standpoint, the creation of an alpha field could increase the effective dose received by the wearer and is generally not recommended. Some forms of radiochromic film have large hydrogen concentrations and show moderate response to neutron radiation [2]. Hydrogen atoms interact with neutrons through elastic scattering events and create detectable recoil protons which deposit energy locally. Hydrogen atoms may also undergo capture reactions and emit gamma radiation which propagates energy away from the interaction site. The ^{1}H(n,γ)^{2}H reaction causes the quality of neutron radiation to change dramatically with depth through tissue as the neutron spectrum degrades and dose from capture photons becomes increasingly more important. Because the quality of radiation changes rapidly, accurate knowledge of a neutron-gamma spectrum is often not feasible [5]. Other possible neutron-tissue interactions include oxygen and carbon elastic scattering, though their importance to absorbed dose is minimal [5]. The DNA dosimeter contains water with single strands of DNA throughout, and has a similar hydrogen fraction to that of tissue (0.112 or 0.102 by weight, respectively) [3]. This enables the DNA dosimeter to scatter and interact with neutron radiation as if it were tissue. Further, the sensitivity of the DNA dosimeter to neutron radiation is also consistent with that of that other radiation. This has been shown by microdosimetric MC algorithms such as *partrac*

which simulate radiation tracks on the molecular level [4]. These MC algorithms have shown that the yield of DNA single strand breaks (SSB) per Gray (Gy) is nearly constant for all radiation types. It should be noted that the number complex double strand breaks is not constants for all types of radiation. The DNA dosimeter responds to ionizing radiation by releasing photons as the DNA single strands are broken. Accordingly, the response of the DNA dosimeter is consistent for all radiation including neutron-gamma fields. A dosimeter's response to ionizing radiation in a mixed neutron-gamma field is broken into two components [6]:

$$R_D = \varepsilon_N D_N + \varepsilon_\gamma D_\gamma \tag{1}$$

Here, R_D is the response of the dosimeter, D_N and D_γ are the respective doses from neutron and gamma radiation, and ε_N and ε_γ are the efficiencies of the dosimeter to measure each radiation type. If the neutron and gamma efficiencies are equal ($\varepsilon_N = \varepsilon_\gamma = \varepsilon$), Equation (1) is simplified:

$$R_D = \varepsilon D_D \tag{2}$$

where D_D is the absorbed *dose-to-dosimeter* and equal to the summation of D_N and D_γ. Under the condition of equal response efficiency (as is the case for the DNA dosimeter) the quantity D_D is easily obtained from Equation (2). If the efficiencies are not equal it is difficult to determine *dose-to-dosimeter* because the response in Equation (1) must be deconvolve. The previously mentioned MC microdosimetric algorithms have determined that the yield of SSB in a water-DNA system is 2.2 ± 0.2 SSB·Gy^{-1} per atomic mass unit of DNA for a wide range of particle types [4]. Thus, in assuming the DNA dosimeter responds with equal sensitivity to all radiation introduces a relative measurement uncertainty of 0.09 at one standard deviation. When considering only ionizing photon radiation, the relative measurement uncertainty is 0.03 at one standard deviation. These values will be used in section 2.2 to determine the total uncertainty of *dose-to-tissue* calculations.

2.2   *Dose-to-tissue* vs. *dose-to-detector*

A personal monitoring dosimeter measures absorbed dose to the specific material present in the active volume of the dosimeter (D_D). However, the quantity of interest in personal monitoring is absorbed *dose-to-tissue* (D_T). To calculate the desired quantity D_T from the measured quantity D_D, a scaling factor derived from fundamental first principals is applied. The scaling factor depends on the radiation type and energy, and if the radiation field is not well characterized, scaling between D_D and D_T may lead to large calculation error. The calculation is further complicated for a mixed radiation field if the dosimeter's response to the different particles is not constant and no method to deconvolve the signal is available (section 2.1).

In personal monitoring, diodes offer the distinct advantage of real-time signal response and can immediately alert the wearer if unexpected radiation is present. However, the active volume is typically silicon (Z = 14.0) and not consistent with tissue (Z = 7.64), leading to large errors when scaling between D_D and D_T. Typically, diodes are used in addition to other personal dosimeters to alert the wearer of possible dangerous radiation fields and not for accurate absorbed dose measurements. For quantified absorbed dose measurement, LiF TLDs and radiochromic film are the industry standard. They are considered tissue equivalent (Z = 8.31, 6.98 for LiF TLDs and

radiochromic film, respectively) though not capable of real-time measurements [2, 3]. Tissue equivalency implies the scaling factor is less dependent on particle type and energy. Dose absorbed by the active volume of a dosimeter is converted to *dose-to-tissue* by scaling with the mass stopping power ratio (S/ρ) of the buildup material B to active volume material in the dosimeter D and the ratio of mass energy absorption coefficients K in the buildup region and tissue [6]:

$$D_T = \left(\frac{\overline{\overline{S}}}{\rho}\right)_D^B K_B^T D_D \tag{3}$$

$$\left(\frac{\overline{\overline{S}}}{\rho}\right)_D^B = \frac{\int_{E_{\min}}^{E_{\max}} \left(\frac{d\Phi}{dE}\right)_B \left(\frac{S_{ion}(E)}{\rho}\right)^B dE}{\int_{E_{\min}}^{E_{\max}} \left(\frac{d\Phi}{dE}\right)_D \left(\frac{S_{ion}(E)}{\rho}\right)^D dE} \tag{4}$$

$$K(\gamma)_B^T = \frac{\left(\mu_{en}(E)\big/\rho\right)^T}{\left(\mu_{en}(E)\big/\rho\right)^B} \tag{5}$$

$$K(n)_B^T = \frac{k_T}{k_W} \tag{6}$$

E is the energy of the primary particle, Φ is the particle fluence, ρ is the mass density, $K(\gamma)$ is the ratio of mass-energy absorption coefficients (μ_{en}/ρ) for gamma radiation, and $K(n)$ is the ratio of neutron kerma factors k. It is clear from Equations (3)-(6) that calculation of D_T requires knowledge of the radiation energy spectrum if the active volume and buildup materials are different from tissue. Figure 1 plots Equation (5), the ratio of mass-energy absorption coefficients in photon radiation, for common personal monitoring dosimeters and the DNA dosimeter. The scaling factor for a diode varies the most because silicon $(Z = 14)$ is the least tissue equivalent of the dosimeters. In the lower energy range, photoelectric events dominate and the mass-energy absorption coefficient is proportional to $Z^{3.3}$, leading to a high scaling factor for radiochromic film $(Z = 6.9)$ and a low scaling factor for LiF TLDs $(Z = 8.31)$. In the therapeutic energy range (0.5 - 20 MeV), Compton events dominate and the mass-energy absorption coefficient is proportional to electron density. Electron density is nearly constant for tissue materials with the exception of hydrogen which has a Z/A ratio of 1. Thus, the LiF TLD, with no hydrogen present, has a scaling factor greater than unity in the therapeutic energy range. Radiochromic film and the DNA dosimeter have a hydrogen content similar to tissue, and the scaling factor is close to unity in the therapeutic range [3]. From Figure 1, the relative error that would result from assuming the *dose-to-dosimeter* is equal to *dose-to-tissue* in Equation (5) is approximately 250%, 200%, and 20% for the silicon diode, radiochromic film, and LiF TLD, respectively. This does not include the errors which would arise from a similar assumption of Equations (4) and (6).
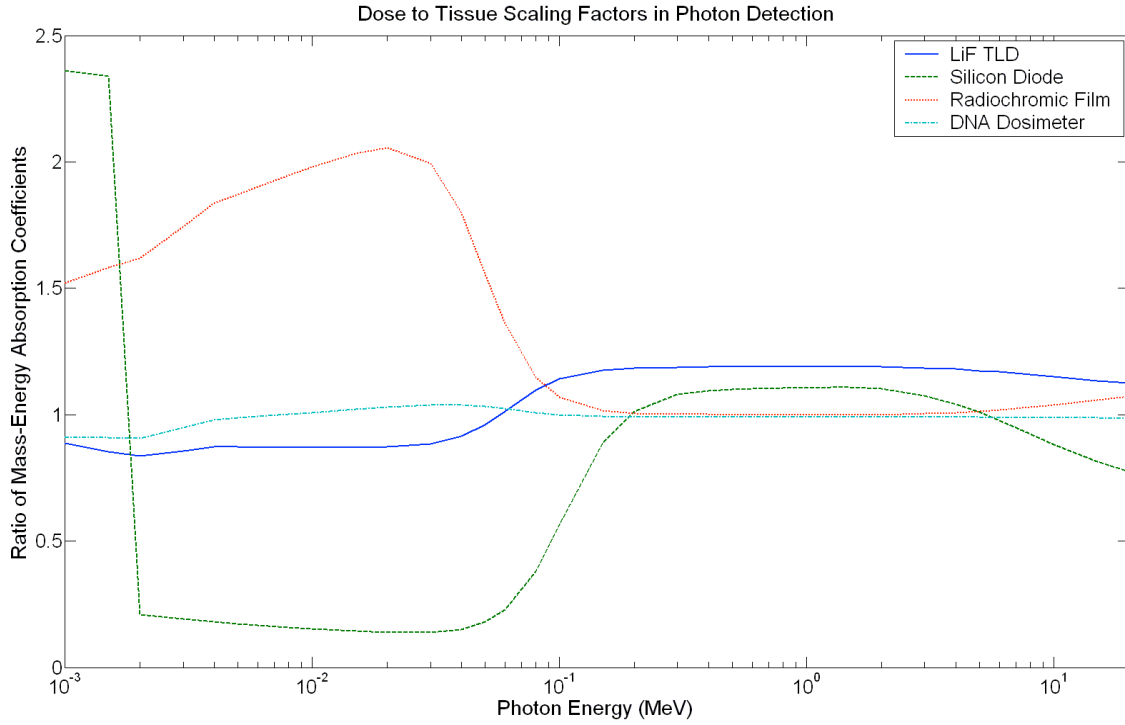
Figure 1 *Dose-to-tissue* scaling factors for photon detection as described by Equation (5)
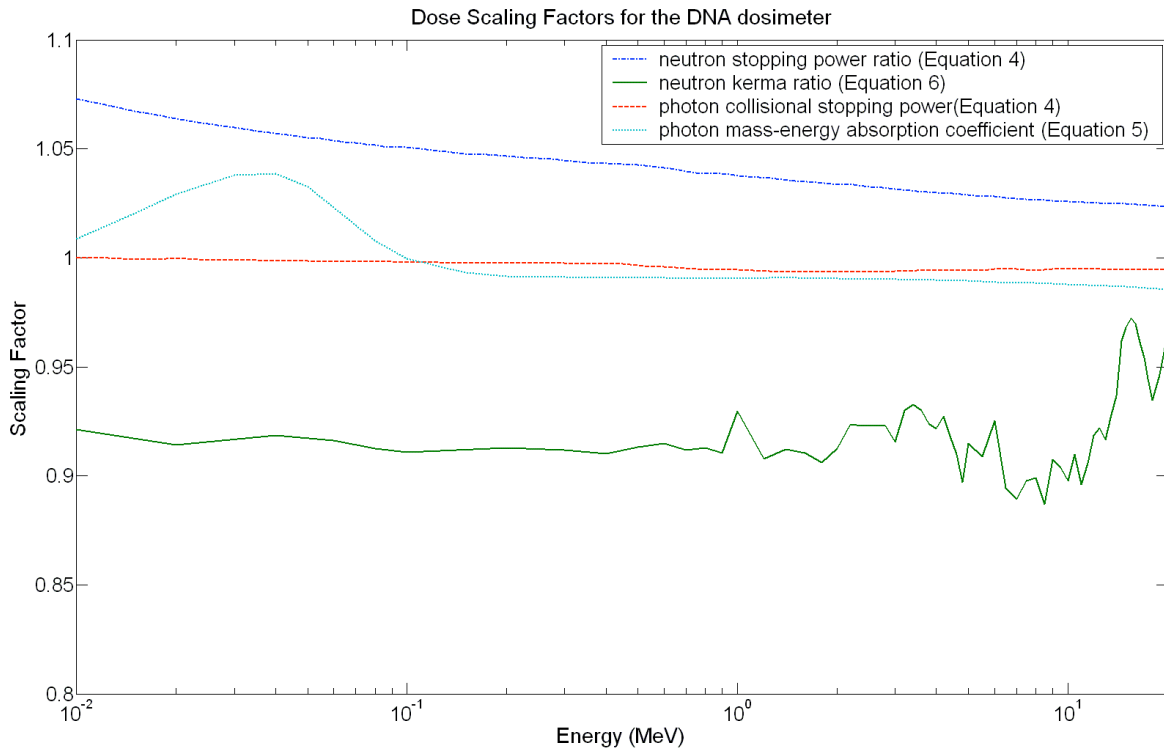

Figure 2 *Dose-to-tissue* scaling factors for the DNA dosimeter

Figure 2 plots all of the required scaling factors for the DNA dosimeter in a broad spectrum of neutron-gamma fields. The stopping power ratio of Equation (4) has been approximated by the ratio of stopping powers:

$$\left(\frac{\bar{\bar{S}}}{\rho}\right)_D^B \approx \frac{\left(S/\rho\right)_B}{\left(S/\rho\right)_D} \tag{7}$$

This approximation is appropriate in a Bragg-Gray cavity where the size of the active volume is negligible compared to the mean range of the scattered charged particles and is applicable to the DNA dosimeter in the energy range plotted [6]. From Figure 2, the neutron scaling factors introduce the largest variation from unity. The neutron stopping power ratio (assumed to result from a field of recoil protons) is greater than zero because the DNA dosimeter has a slightly lower effective atomic number than tissue (7.51 vs. 7.64, respectively) and the stopping power of heavy charged particles is proportional to Z^2 [3]. The neutron kerma ratio is slightly less than unity because the DNA dosimeter has a larger hydrogen component than tissue and elastic scattering with hydrogen is the primary neutron interaction in tissue. The photon collision stopping power (assumed to result from a field of delta rays) is near unity throughout the spectrum because the electron stopping power is not a function of material composition. The ratio of mass-energy absorption coefficients is slightly above unity in the photoelectric region because the DNA dosimeter's effective atomic number is slightly less than that of tissue. The absorbed *dose-to-tissue* is calculated with Equations (3)-(6):

$$D_T = \left(\frac{\bar{\bar{S}}}{\rho}\right)_\gamma K_\gamma D_{D-\gamma} + \left(\frac{\bar{\bar{S}}}{\rho}\right)_n K_n D_{D-n} \tag{8}$$

where the neutron and gamma contributions have been separated. With the DNA dosimeter, calculation of D_T requires the assumptions that each scaling factor in Equation (8) is equal to unity. From Figure (2), the assumption of unity introduces the following uncertainties:

$$\left(\bar{s}/\rho\right)_\gamma = 1.00 \pm 0.01$$
$$\left(\bar{s}/\rho\right)_n = 1.00 \pm 0.06$$
$$K_\gamma = 1.00 \pm 0.03$$
$$K_n = 1.00 \pm 0.08$$

Following a standard error propagation calculation, the relative uncertainty for gamma radiation including the measurement uncertainty (0.03) from section 2.1 is 0.04, the relative uncertainty for neutron radiation including the measurement uncertainty (0.09) is 0.13, and the net uncertainty for the DNA dosimeter to measure *dose-to-tissue* is 14% for mixed neutron-gamma fields. This derivation is conservative because the majority of the uncertainty comes from the two neutron scaling factors which have opposing effects and most likely cancel.

3.   The DNA dosimeter

The DNA dosimeter responds to ionizing radiation by releasing visible photons. The photons are released due to a rapid decrease in the probability of Förster Resonance Energy Transfer as DNA strands break (see section 3.1). The number of photons released is linearly proportional with number of DNA strands broken (section 2.1), and the number of single DNA strands broken is linearly proportional with dose (section 3.2) for all radiation types. Linearity has been experimentally verified from 0.1 to 10 Gy in x-ray and gamma fields, and the lower limit of detection for the DNA dosimeter is 100 mGy.

3.1   Förster Resonance Energy Transfer

The DNA dosimeter designed at the Royal Military College of Canada is fundamentally based on the physics of Förster resonance energy transfer (FRET). FRET is a mechanism in which molecular electronic excitation energy of a reporter molecule is redistributed to neighbouring quencher molecules through non-radiative dipole-dipole interactions. The fraction of excitation energy transferred to neighbouring molecules (termed FRET efficiency or P_{FRET}) is highly dependent on the distance between the reporter and quencher, and rapidly drops to zero as they separate. Before the DNA molecule is exposed to ionizing radiation, the single strand of DNA tethers the reporter and quencher close together. In this case, FRET efficiency is close to unity and excess reporter energy is transferred to the quencher and dissipated as heat. After exposure to ionizing radiation, the DNA strand breaks allowing the reporter and quencher to drift apart. In this case, the FRET efficiency drops to zero and excess reporter energy is converted into a visible photon. The probability of a FRET event has been derived elsewhere [7]. It is a function of the radiative lifetime τ_o, distance between the reporter and quencher molecules R, and the Förster parameter R_o:

$$P_{FRET} = \frac{1}{\tau_o}\left(\frac{R_o}{R}\right)^6 \tag{9}$$

The Förster parameter characterizes the strength of dipole-dipole interaction energy and contains information about the spectral overlap between emission and absorption spectra:

$$R_o \propto \left(\int \frac{f_D(\omega)\sigma_A(\omega)}{\omega^4}d\omega\right)^{1/6} \tag{10}$$

where ω is the angular frequency, f_D is the normalized emission spectra of the reporter molecule, and σ_A is the is the absorption cross section of the quencher molecule. From Equation (9) it can be seen that a small increase in the separation distance R results in a rapid decrease in the probability of a FRET event. Thus, when ionizing radiation breaks the DNA strand, the probability of a FRET event rapidly drops to zero. When FRET does not occur, a visible photon is released to dissipate the excess energy.

Figure 3 Possible scenarios after the DNA dosimeter is exposed to ionizing radiation.
R represents the reporter molecule and Q represents the quencher molecule.

3.2   Linearity

The DNA molecule works as a switch: resting in the off position while the molecule is intact, and turning on after ionizing radiation breaks the DNA strand. The DNA strand tethers the donor and acceptor chromophores close together, allowing P_{FRET} of the molecules to undergo FRET (switch off). Ionizing radiation breaks the DNA strand and the donor and acceptor drift apart to reach an equilibrium state. Due to the R^{-6} energy transfer dependence in Equation (9), $P_{FRET} \rightarrow 0$ as the reporter and quencher separate. In this case, the molecular electronic excitation energy of the reporter is converted to a visible photon (switch on). If the system contains N DNA molecules and the number of single strand breaks is proportional to absorbed dose D (section 2.1), the number of undamaged and damaged molecules (N_u and N_d respectively) can be expressed according to the following equations:

$$N_u = N(1 - \beta D) \tag{11}$$

$$N_d = N\beta D \tag{12}$$

where β is the proportionality constant governing linearity between dose and strand breaks and approximately equal to 2.2 ± 0.2 SSB·Gy^{-1} per atomic mass unit of DNA [4]. Figure 3 depicts the four possible scenarios following exposure to ionizing radiation: (1) the molecule is undamaged and FRET occurs, (2) the molecule is undamaged and FRET does not occur, (3) the molecule is damaged and FRET occurs, and (4) the molecule is damaged and FRET does not occur. The number of molecules in each scenario can be described by the following equations:

$$N_1 = N(1 - \beta D)P_{FRET} \tag{13}$$
$$N_2 = N(1 - \beta D)(1 - P_{FRET}) \tag{14}$$
$$N_3 = N\beta D P_{D-2} \tag{15}$$
$$N_4 = N\beta D(1 - P_{D-2}) \tag{16}$$

where P_{D-2} is the probability of a secondary FRET event (case 3). Cases 2 and 4 lead to the emission of a photon and their sum is the total number of photons released N_γ:

$$N_\gamma = N_{\gamma o} + N\alpha D \qquad (17)$$

where $N_{\gamma o} = N(1\text{-}P_{FRET})$ is the number of photons emitted before exposure and $\alpha = \beta(P_{FRET}\text{-}P_{D-2})$ is the rate of change in photon count with dose and has units of Gy^{-1}. Equation (17) shows the linear relationship between the probability of a photon emission and dose. In deriving this equation it was assumed reporter and quencher molecules do not lose the ability to fluoresce/absorb with dose. This assumption has been verified during the experimental phase of testing in section 3.3.

3.3   Experimental Verification

Preliminary experiments were conducted to validate the DNA dosimeter theory. The goal of the experiments was to show a linear relationship between photon count and radiation dose, determine if any radiation related degradation of the donor and acceptor exists, and determine a lower limit of detection. Two initial experiments were conducted. The first set of samples was irradiated at Defence Research and Development Canada (DRDC) in Ottawa, Ontario. Radiation was delivered from a cobalt-60 source which decays to an excited state of nickel-60 via beta emission, and subsequently releases two gamma rays of 1.17 and 1.33 MeV. Dose levels for the first experimental set ranged from 0.1 to 10 Gy. The second set of samples was irradiated by a 6 MV linear accelerator (linac) at the Kingston General Hospital. In a linac, electrons accelerate through a 6 MV potential and gain 6 MeV of energy as they reach a gold or tungsten target, creating a spectrum of x-ray photons with a maximum energy of 6 MeV. Dose levels for the second set of irradiations ranged from 0.01 to 10 Gy. For both experiment, each data point was done in triplicate. The results from each experiment are plotted in Figure 4. A linear best-fit line has been added for each data set and was calculated using a weighted least-squares method. Both sets of results confirm the linear relationship between fluorescence signal and dose, and from a regression analysis with a 95% confidence limit, the slopes from these experiments give similar dose response. This confirms the system response is similar for the two different radiation fields validating the hypothesis is section 2.1, and that the response is linear with dose as described in Equation (17). From these experiments the lower limit of detection was 100 mGy.

Figure 5 depicts the quencher molecule's response with dose. This experiment was designed to determine if the quencher degrades in a radiative field and if the assumption in deriving Equation (17) is valid. The experiment was performed by the measuring the quencher's absorbance after being exposed to various dose levels. The absorbance cross section is the quencher characteristic which affects the probability of a FRET event according to Equations (9) and (10). Absorbance was calculated by passing a 535 nm photon beam through solution and measuring the transmitted beam intensity, where 535 nm corresponds to the maximum emission frequency of the reporter molecule. According to a χ^2 test with a 95% confidence level, there is no significant degradation of the quencher molecule for 0 to 5 Gy of radiation.
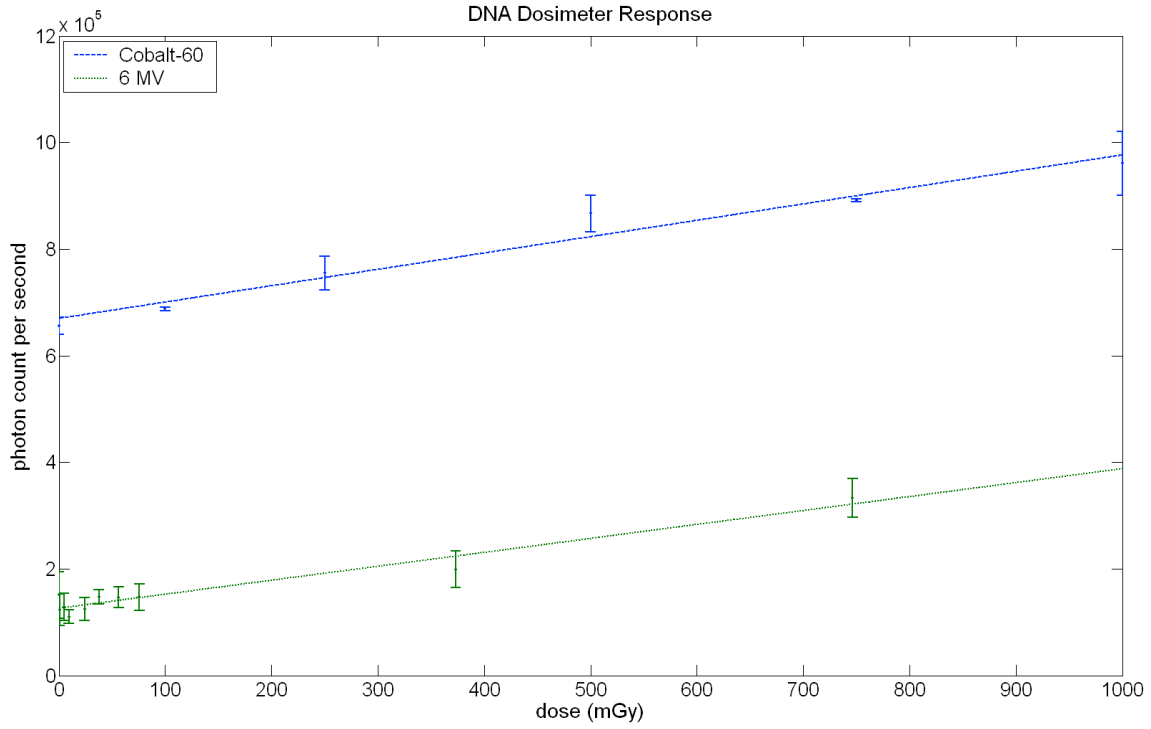
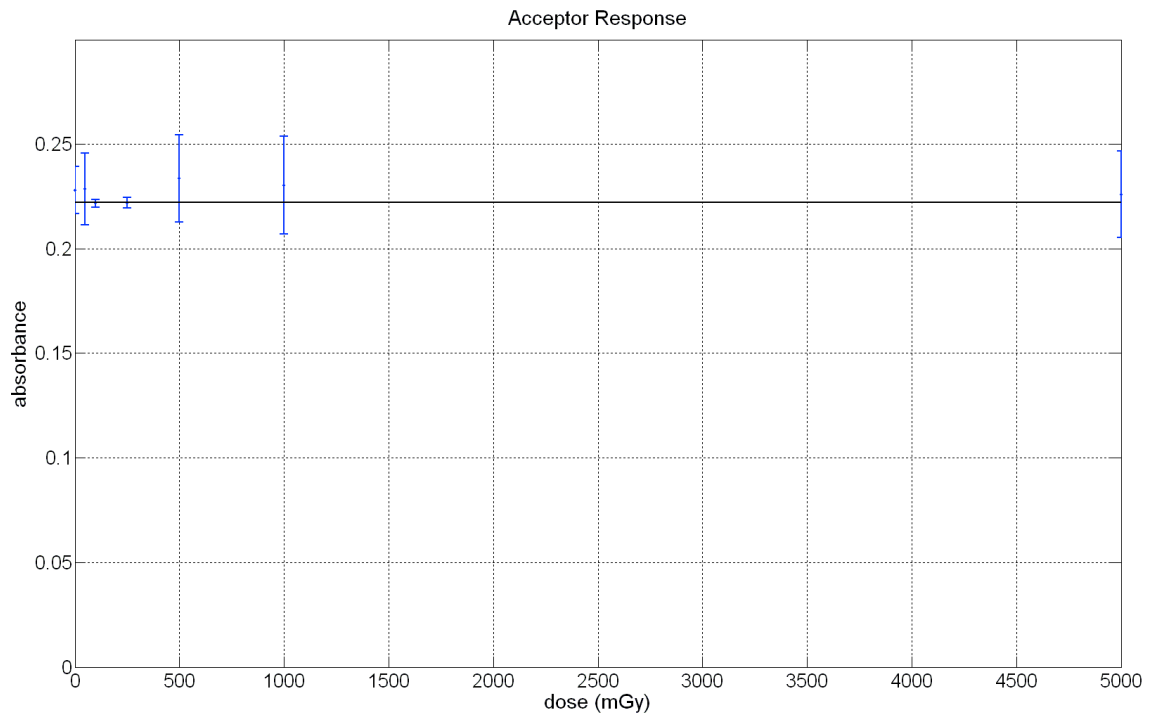Figure 4 Linear response of the DNA dosimeter in X-ray and gamma fields

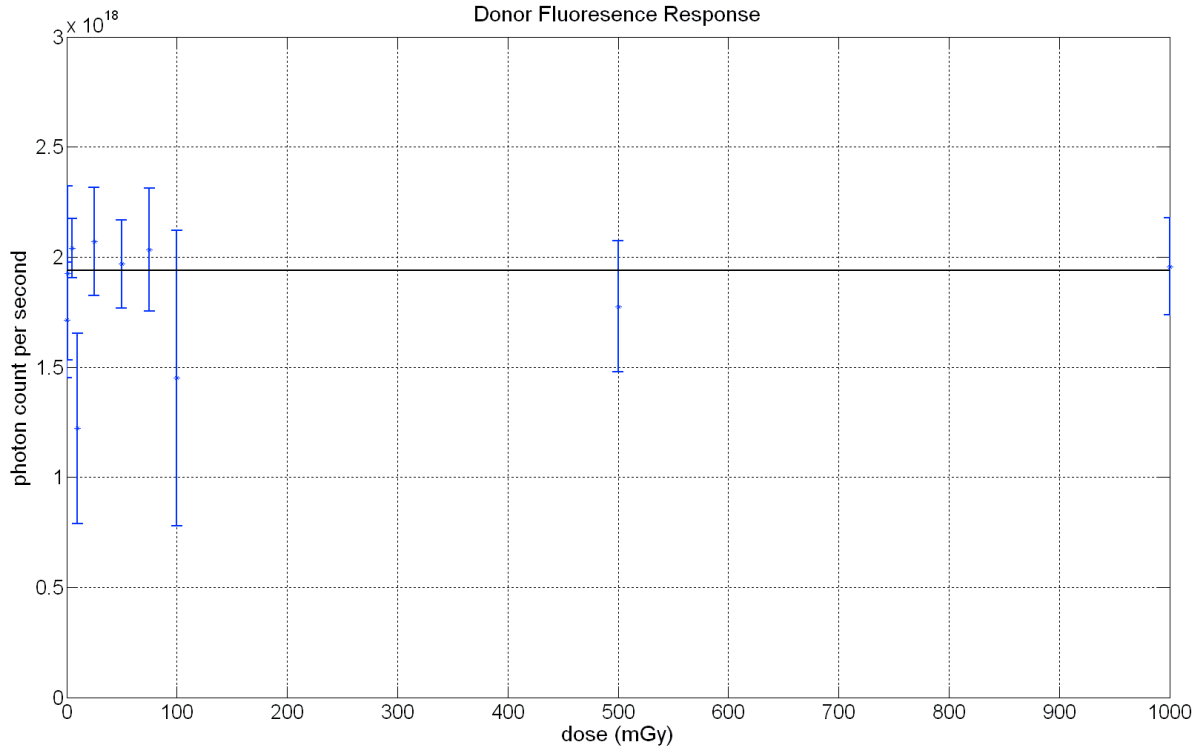Figure 5 Test for degradation of acceptor *A* with dose

Figure 6 Test for degradation of donor *D* with dose

Figure 6 shows the reporter's fluorescence response with dose, an experiment performed to determine if the molecule is degrading in a radiative field. The data points were obtained by measuring the fluorescence response of a serial dilution at various dose levels. The slope from each dilution set is plotted versus dose in Figure 6. The results show no significant degradation in the reporter molecule with dose up to 1 Gy according to a χ^2 test with a 95% confidence level. The results of these preliminary experiments were important to validate the theoretical model of the DNA dosimeter (section 3.2) and the linearity prediction of Equation (17).

4.   Summary

A novel DNA dosimeter designed at the Royal Military College of Canada is capable of accurate absorbed dose measurements in mixed neutron-gamma fields for personal monitoring purposes. The active volume of the dosimeter contains hydrogen and is theoretically capable of responding to neutron radiation field. In contrast, other common personal monitoring devices such as LiF TLDs and silicon diodes typically do not respond to neutron radiation. The DNA dosimeter is tissue-equivalent and the *dose-to-detector* can be interpreted as *dose-to-tissue* with 14% accuracy in any mixed neutron-gamma field. The DNA dosimeter theory has been experimentally verified, with the results showing a statistically similar response in two different photon fields. The lower limit of detection is 100 mGy and there is no statistically significant degradation of the reporter or quencher molecules below dose levels of 1 Gy.

5. Acknowledgements

6. Funding

7. References

[1]   The Canadian Nuclear Safety Commission, "Nuclear safety and controls act", Minister of Justice, 2010

[2]   S.L. Brady, R. Gunasingha, T.T Yoshizumi, C.R. Howell, A.S. Crowell, B. Fallin, A.P. Tonchev, and M.W. Dewhirst, "A feasibility study using radiochromic film for fast neutron 2D passive dosimetry", Phys Meb Biol Vol 55, 2010, pp.4977-4992

[3]   H.E. Johns and J.R. Cunningham, "The Physics of Radiology", Charles C Thomas, 4th edition, 1983

[4]   H. Nikjoo, P. O'Neill, M. Terrissol, and D.T. Goodhead, "Quantititive modeling of DNA damage using Monte Carlo track structure method", Radiat Environ Biophys, Vol 38, 1999, pp.31-38

[5]   F.H Attix and W.C. Roesch, "Radiation Dosimetry", Academic Press, 2nd edition, Vol. 1, 1968

[6]   P. Almond, F.H. Attix, M. Awschalom, P. Bloch, J. Eenmaa, L. Goodman, R. Graves, J. Horton, F. Kuchnir, J. Mcdonald, V. Otte, P. Shapiro, J. Smathers, N. Suntharalingham, and F. Waterman, "Protocol for neutron beam dosimetry", American Association of Physicists in Medicine, Report No. 7, 1980

[7]   T. Wood, B.J. Lewis, K. McDermott, L.G.I. Bennett, K. Avarmaa, E.C. Corcoran, D. Wilkinson, A. Jones, T. Jones, E. Kennedy, L. Prud'homme-Lalonde, D. Boudreau, J.-F. Gravel, C. Drolet, A. Kerr, L.J. Schreiner, M. Pierre, R. Blagoeva, T. Veres, "Use of a Dual-Labelled Oligonucleotide as a DNA Dosimeter for Radiological Exposure Detection", Radiat Prot Dosim, Vol. 143, Iss. 2, 2011